



<https://doi.org/10.33003/fjorae.2025.0201.02>

DEGRADATION OF TiO_2 ANTIREFLECTION COATINGS: THERMAL AND MECHANICAL STRESS EFFECTS OVER 35 YEARS

¹S. D. Muhammad¹ and M. H. Ali²

National Environmental Standards Regulations and Enforcement Agency, Department of Physics, Bayero University, Kano

Abstract

This study investigates the effects of 35 years of thermal and mechanical stress on titanium dioxide (TiO_2) antireflection coating, as well as the TiO_2 /GaAs interface. The analysis was conducted using the COMSOL Multiphysics environment, employing heat transfer in solids and structural mechanics models to evaluate key parameters under the temperature range of -40°C to 140°C and load of 10N, including the first principal stress, surface emissivity, TiO_2 /GaAs interface toughness, deformation gradient, and crack growth direction. The findings reveal that during the first five years under the specified thermal and mechanical boundary conditions such as surface-to-ambient radiation, fracture mechanic, convective heat transfer etc, the first principal stress at the coating surface and interface decreased to 0.07MPa and 0.08MPa, respectively, while the deformation gradient exhibited negligible changes. However, between 5 and 20 years, a sharp increase in stress was observed, with values rising to 0.14MPa at the surface and 0.19MPa at the interface. The significant deformation gradient resulted in a reduction of surface emissivity from 0.9 to 0.3 and a decline in interface toughness from 0.25MPa to 0.01MPa. A crack growth direction magnitude of 0.83% was detected, particularly at both the coating edges and interface. Between 20 and 35 years, both the stress and deformation gradient increased gradually, gesturing that the coating could no longer withstand additional stress at this stage. These results provide valuable insights into failure mode analysis during the practical stress testing of photovoltaic modules, aiding in the assessment of long-term performance and reliability.

Keywords: Antireflection coating, COMSOL Multiphysics, Deformation gradient, Titanium dioxide, Photovoltaic module,

INTRODUCTION

The reliability and lifespan of photovoltaic (PV) modules are influenced by their construction, manufacturing processes, and the environmental conditions in which they are installed (Owen-Bellini *et al.*, 2021a). PV modules are subject to various degradation modes, including Ethylene Vinyl Acetate (EVA) discoloration, delamination, glass and cell breakage, junction box damage,

¹ sunusidayab@gmail.com, mhali.phy@buk.edu.ng

and corrosion of metallic components. These degradation modes are primarily driven by harsh outdoor environmental factors such as temperature, humidity, rainfall, snow, hail, wind, and dust (Namvar *et al.*, 2016). These conditions contribute to reduced power output, efficiency, and overall lifespan of the modules (Leem *et al.*, 2014).

To enhance the efficiency and longevity of PV modules, manufacturers often deposit antireflection coatings (ARCs) on the front glass using techniques such as spin coating, sol-gel, dip coating, and vapor deposition. Materials like silicon dioxide (SiO_2), magnesium fluoride (MgF_2), aluminum oxide (Al_2O_3), and titanium dioxide (TiO_2) have been explored for ARC development to improve optical performance and durability. Among these, TiO_2 stands out due to its superior optical and mechanical properties, including a high refractive index, Young's modulus, thermal conductivity, and thermal expansion coefficient (Raquel & Angelo, 2016; Rezaei & Mosaddeghi, 2006). These attributes make TiO_2 highly suitable for designing durable single-layer or multilayer ARCs. However, the durability of ARCs depends significantly on the interaction between the coating and the substrate (Jorgensen *et al.*, 1999). These interactions can be homogeneous, where the coating and substrate share similar physical properties such as intermolecular bonding, hardness, and flexibility, or nonhomogeneous, where there are significant differences between their physical properties. Under outdoor conditions involving temperature fluctuations, humidity, and precipitation, the long-term interaction between the coating and substrate can impact the PV module's durability (Noman *et al.*, 2022).

Previous research and industry reports indicate that PV modules are designed to withstand outdoor conditions for 20 to 35 years (Noman *et al.*, 2022; Owen-Bellini *et al.*, 2021b). To ensure this durability, the International Electrotechnical Commission (IEC) has developed standards, such as IEC 61215 and IEC 61646, which involve laboratory tests simulating outdoor conditions, including 1,000 hours of damp heat at 85°C and 85% relative humidity (Arndt & Robert Puto, 2010; IEC, 2008.). However, previous studies (Gambogi *et al.*, 2015; Kempe *et al.*, 2023; Wohlgemuth & Kempe, 2020) on ARCs have mostly focused on short-term conditions, that, whereas this study addresses long-term degradation.

Several studies have contributed to this understanding. Eitner *et al.*, (2011) quantified the thermomechanical stresses in a 60-cell PV module without ARC using finite element analysis, finding that the non-symmetrical structure of the 5.55mm thick module, with front glass as the thickest component, caused bending effects during thermal cycling. Hasan *et al.*, (2014) conducted a life prediction analysis of PV modules without ARC, revealing that copper interconnects undergo plastic deformation shortly after the lamination process, with an average lifespan of 26.5 years under Saudi Arabian outdoor conditions. Noman *et al.*, (2022) analysed PV modules without ARC operating for 10 to 35 years at Pakistan's oldest PV installation site, identifying degradation modes such as junction box damage, cracking, discoloration, and

delamination, all contributing to reduced power output and efficiency. Recent studies on ARC development have shown promising results. Zeng *et al.*, (2023) fabricated and characterized open-pore and dense silica ARCs and subject it under short-term outdoor conditions. The results demonstrating that while dense ARCs exhibit better stress resistance, open-pore ARCs provide longer lifespans, albeit with reduced optical performance. Zäll *et al.*, (2023) evaluated the optical and mechanical durability of closed-pore silicon dioxide ARCs under various durability tests, finding superior mechanical durability in humidity freeze and industrial climate chamber conditions. However, the aforementioned studies were evaluated under short-term test conditions where the ARCs revealed early mode degradation.

In this study, first principal stresses, toughness at the coating/substrate interface, surface emissivity, deformation gradient, and crack growth direction are evaluated under thermal and mechanical loads over 35 years using COMSOL Multiphysics software. The results aim to guide the development of PV modules with improved thermal stability and mechanical strength, contributing to enhanced durability and reliability in outdoor conditions.

Theoretical Background

This research evaluated thermal and mechanical parameters interconnected by established physical theories. Key material properties considered include temperature, stress, strain, Young's modulus, coefficient of thermal expansion, density, and thermal conductivity.

Heat Distribution at the Boundary

When a PV module is exposed to outdoor environments, the ARC interacts with its substrate (solar cells) due to external environmental factors such as temperature, relative humidity, solar radiation, wind, rainfall, hail, and dust. These outdoor parameters affect the coating material's properties such as Young modulus and thermal conductivity. The heat radiated from the sun to the coating surface can be expressed through radiative heat flux, given by (Bharatish *et al.*, 2015):

$$q_{rad} = \epsilon\sigma(T^4 - T_{amb}^4) \quad (1)$$

where q_{rad} is the radiative heat flux (W/m^2), ϵ is the emissivity of the coating surface (dimensionless between 0 and 1), T is the surface temperature (K) and T_{amb} is the ambient temperature (K)

The heat transfer from the coating surface to the surroundings through convection is given by (Białas, 2008):

$$q_{conv} = h(T - T_{amb}) \quad (2)$$

where q_{conv} is the convective heat flux (W/m^2), h is the convective heat transfer coefficient (W/m^2), T is the surface temperature (K) and T_{amb} is the ambient temperature (K)

The total heat flux at the surface, combining radiation and convection, can be expressed as:

$$q_{total} = h(T - T_{amb}) + \epsilon\sigma(T^4 - T_{amb}^4) \quad (3)$$

For the heat flux at the boundary interface, the following equation applies (Haider *et al.*, 2005):

$$q_{total} = -k\Delta T \times n + q_{ext} \quad (4)$$

where k is the thermal conductivity of the materials (W/mK), n is the boundary normal vector, q_{ext} is the external heat at the boundary (W/m^2), and ΔT is the temperature gradient (K/m)

The general temperature distribution at the surface and within the solar module, accounting for conduction, convection, and radiation, requires that Equation (3) equals Equation (4):

$$-k\Delta T \times n + q_{ext} = h(T - T_{amb}) + \epsilon\sigma(T^4 - T_{amb}^4) \quad (5)$$

The transient temperature distribution within the coating can be described by (Moridi *et al.*, 2014):

$$d_z \rho C_p \times \frac{\partial T}{\partial t} = \Delta q \quad (6)$$

Where $\Delta q = -d_z k \Delta T$ is the heat change over time, C_p is the specific heat capacity at constant pressure, ρ is density of the coating material, d_z is the coating thickness and t is the time taken for the heat distribution

Thermal Stress, Strain, and Toughness

Temperature fluctuation is a major environmental factor that can distort the coating, inducing stress or strain. The relationships are expressed as:

$$\epsilon_T = \alpha \Delta T \quad (7)$$

$$\delta_T = E \alpha \Delta T \quad (8)$$

where ϵ_T is the elastic strain energy as a function of temperature, α is the coefficient of thermal expansion, E is the Young modulus of the material, δ_T is the thermal stress and ΔT is the temperature fluctuation.

Excessive thermal stress caused by high temperatures can initiate cracks in the coating. To determine the toughness at the coating/substrate interface, the strain energy stored at the interface is used:

$$\Gamma = \frac{\epsilon_s}{A} \quad (9)$$

where Γ is the toughness between the coating and the substrate, ϵ_s is the strain energy store, and A is the area of the interface.

If the initial toughness is sufficiently high before exposure to outdoor conditions, the coating remains adhesive. However, high thermal or mechanical stress can lead to expansion of the coating and substrate, increasing the coating surface and interface area. This expansion reduces adhesive force and toughness at the surface and interface, potentially leading to cracks and deformation.

Looking at all equations, the temperature variation has significant role in distorting the materials' properties by affecting the atomic and molecular kinetic behaviours.

MATERIALS AND METHODS

The materials of this study involved COMSOL Multi-Physics software, virtual TiO_2 as ARC material, and GaAs solar cell as substrate. Therefore, the thermal and mechanical stress distribution on the surface of a TiO_2 ARC and at the coating/substrate (GaAs) interface can be simulated, considering material properties that vary with temperature and time.

Materials Selection

GaAs solar cell was chosen as the substrate due to their lower thermal and mechanical properties compared to TiO_2 . This contrast in material properties creates a nonhomogeneous interface, critical for studying stress distributions at the coating/substrate boundary.

Most material properties of TiO_2 ARC and GaAs solar cells were obtained from the COMSOL Multiphysics 5.6 material library, as summarized in Table 1. Additional material properties were sourced from relevant literature (Eitner *et al.*, (2011), Parajuli *et al.*, (2023)).

Table 1: Material Properties for TiO_2 ARC and GaAs solar cell

Parameter	GaAs	TiO_2 ARC
Coefficient of thermal expansion	5.8×10^{-6}	8.6×10^{-6}
Thermal conductivity	46W/mK	11W/mK
Young modulus	85GPa	230GPa
Density	5317Kg m^{-3}	4230Kg m^{-3}
Heat Capacity	330J/KgK	690J/KgK
Poisson ratio	0.31	0.27
Bulk modulus	75GPa	180GPa
Shear modulus	39.6GPa	100GPa

Simulation

The simulation was carried out using COMSOL Multiphysics environment, a finite element analysis, solver, and simulation software designed for engineering and scientific applications across various disciplines. This software enables the modelling and simulation of coupled physical phenomena such as structural mechanics, optics, heat transfer, fluid dynamics, electromagnetics, and acoustics. For this study, the Structural Mechanics and Heat Transfer modules were utilized with a time-dependent study to evaluate stress distributions.

The simulation setup involved the following:

- The Model Builder for creating the simulation workflow.
- Settings were used to define material properties, boundary conditions, and study parameters.
- A Graphics Page for visualizing the simulation results.

This methodology ensures accurate modelling of the temperature and time dependent behaviour of the materials, enabling a comprehensive analysis of stress distribution in the TiO_2 ARC and the interface.

The geometrical structure of the model was designed as a two-dimensional rectangular domain for computational simplifications and visualization, as depicted in figure 1. The dimensions of the TiO_2 ARC and GaAs solar cell were set to 80 nm and 300 nm by 100nm, respectively. The boundary conditions applied in the heat transfer model included surface-to-ambient radiation, convective heat flux, and boundary heat source to account for heat transfer mechanisms such as convection, conduction, and radiation at the coating surface, interface, and other parts of the cell.

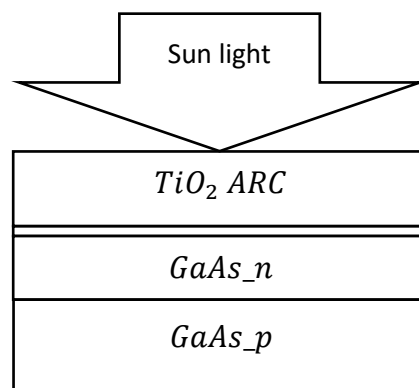


Figure 1: The diagram of GaAs solar cell coated with TiO_2 ARC

To analyse crack growth propagation, fracture boundary conditions, along with thermal and mechanical loads of 10N, were applied. Additionally, to simulate expansion and contraction caused by thermal cycling, a surface emissivity of 0.9 was selected. The temperature range was set between an initial temperature of 25°C and a variable interval of -40°C to 120°C, as reported in relevant literature(Białas, 2008)

In the structural mechanics model, the vertical edges of the domain were designated as free boundaries to prevent domain movement under applied loads (force per unit area). All domains were modelled as linear elastic and isotropic materials. Fixed constraint boundary conditions were applied at the interface, cell junctions, and back contact to identify specific stresses, crack growth directions, and deformation gradients.

For smooth computations and boundary conditions, an extra fine mesh was applied to the TiO_2 ARC layer, while a finer mesh was used for the remaining parts of the structure. The mesh was refined iteratively, up to a maximum of 1,000 iterations, until the desired results were achieved with an error tolerance of 0.5. This process required a physical memory of 974 MB and a minimum computation time of 15 minutes and 30 seconds (15 min, 30 s).

To evaluate the thermomechanical stress distribution, deformation gradient, and crack growth direction, the structural mechanics and heat transfer models were coupled. A thermal expansion interface was created to link the models. The time-dependent study was computed for a simulation period ranging from 1 to 35 years under the applied thermal and mechanical loads. The results were post-processed using the Model Builder, Settings, and Graphics Pages in the software to extract and visualize the outcomes.

RESULT AND DISCUSSION

The 35 years thermal and mechanical stress distribution and deformation gradient on the toughness of the TiO_2 ARC/GaAs solar cell interface, as well as the surface emissivity of the coating, has been evaluated

First Principal Stress Distribution and Deformation Gradient at coating Surface

Photovoltaic modules are designed to last for 25 to 35 years, corresponding to the warranty period offered by manufacturers. However, these modules experience chemical and thermomechanical stresses due to seasonal and daily temperature variations. Figure 2 illustrates the thermal stress distribution on the surface of the TiO_2 ARC during the first five years under thermal and mechanical load, that is boundary conditions of surface-to-ambient radiation with an emissivity of 0.95, heat boundary conditions with temperature variations ranging from 25°C to 150°C.

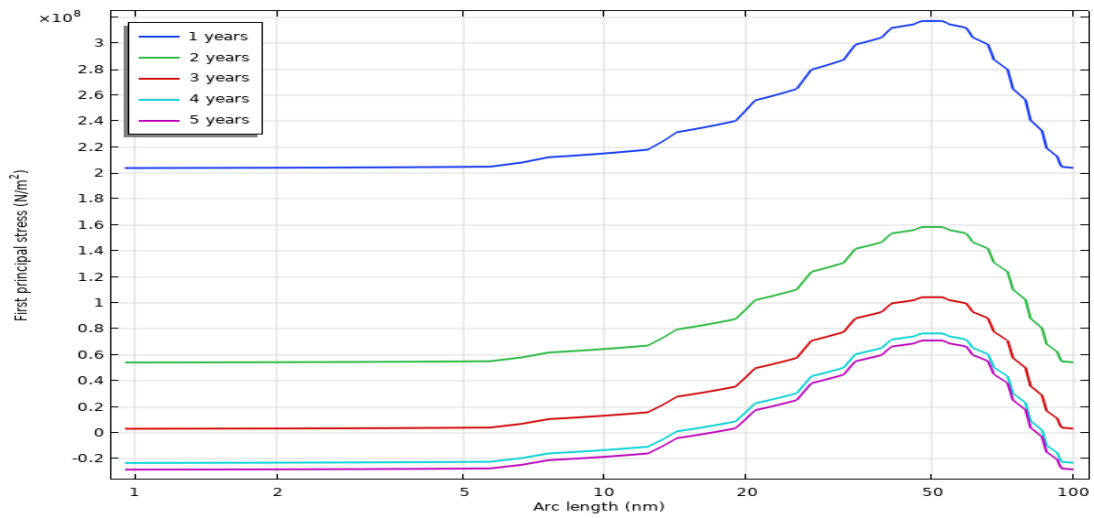


Figure 2: 5-years First principal stress at surface of TiO_2 ARC

From figure 2, the first principal stress showed a significant decrease from 0.32MPa to 0.078MPa over the first four years, followed by a gradual decline with a smaller gradient of 0.008MPa until the fifth year with 0.07MPa. This indicates that at the arc length of 50nm, the tensile stress occurred due to stress relaxation and strain redistribution induced in the coating particles during the loads applied. Fatigue was identified as the primary defect within this period, attributed to the low thermal stress cycle. However, after five years, the stress began to increase as shown in figure 3.

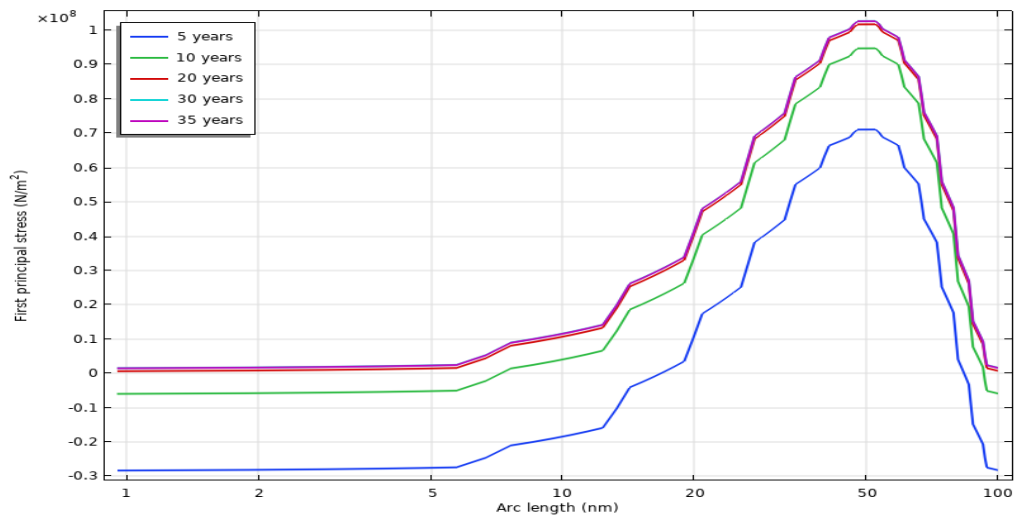


Figure 3: 35-years First principal stress distribution at surface of TiO_2 ARC

Examining figure 3, an abrupt increase in principal stress was observed between 5 to 20 years, reaching 0.14MPa and from 20 to 35 years, there was a gradual increase of 0.001 MPa per year. Over time, the coating material loses its elastic properties due to stress cycling, leading to the

development of cracks and other defects within the coating, which deforms it to the point of failure. Consequently, it can no longer resist the applied stresses.

In practice, the coating is usually deposited at a high temperature of about 300°C and allowed to cool rapidly (Yu & Cen, 2017). During this process, the coating particles are positioned and arranged in a specific order. However, due to thermal stress cycling and prolonged exposure, the particles shift and become arranged both interstitially or substitutionally. As a result, the coating does not experience persistent deformation in the short term as also observed in this work. But after a long-term exposure, deformation becomes dominant at the most stressed points, as shown in figure 4.

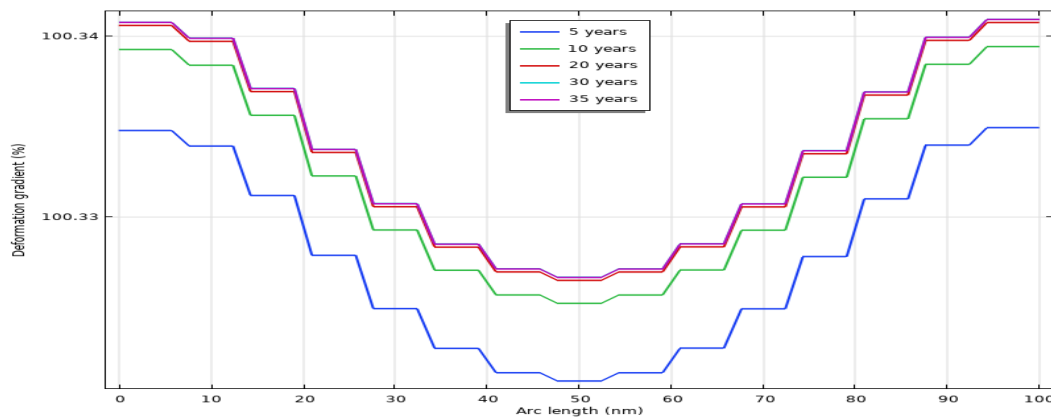


Figure 4: 35-years deformation gradient at the surface of TiO_2 ARC

Repeated expansion and contraction over an extended period alter the coating's structure, significantly affecting its service life. The coating surface deformation initiates failure modes such as cracking and discoloration at areas where thermal stress is concentrated. Repeated high temperature of 120°C experienced by the coating surface for 35 years, reduce the elastic nature of the surface and result the surface emissivity to decrease from 0.95 to 0.30 which cause retention of more heat at the coating surface. The dislocation of particles and imperfection at the stressed regions initiated the cracks where the subsequent thermal stress increased which raised the crack growth rate to 0.83% from 0.01%. Consequently, it also causing thermomechanical stress to transfer to the coating/substrate interface and, eventually, to other components of the PV module.

4.1. First Principal Stress Distribution and Deformation Gradient at Coating Interface

The interface between the coating and the substrate is a critical area that needs to be strengthened in order to reduce thermal and mechanical stresses. It is well known that the level and distribution of thermal stress at the coating interface significantly impact the coating's lifespan then mechanical load (Yu & Cen, 2017). Therefore, one of the main factors contributing to thermomechanical stresses at the interface is the difference in the coefficients of thermal

expansion. Figure 5 illustrates the first principal stress at interface under five years of exposure. During this period, the first principal stress decreases from 0.24 MPa to 0.08 MPa uniformly between the arc length of 15nm and 70nm, causing the minimum compressive stress to dominate the interface.

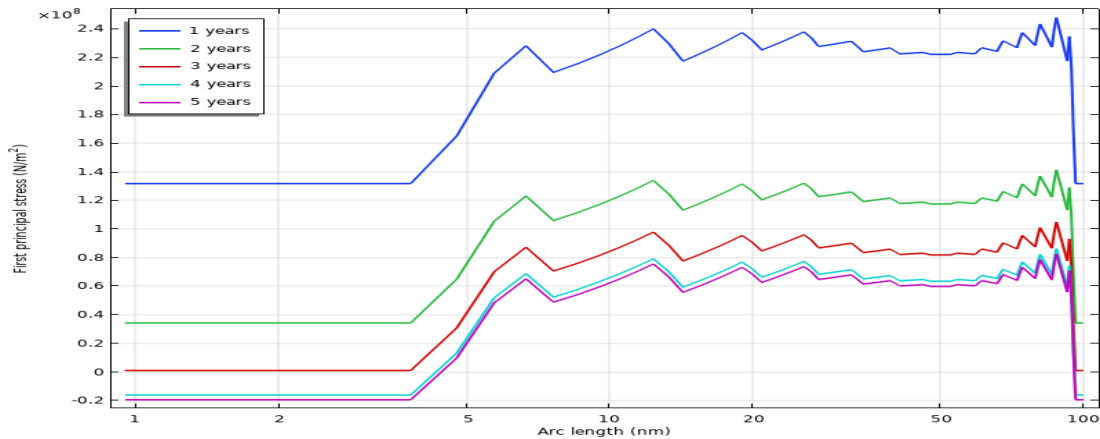


Figure 5: 5-years first principal stress distribution at TiO_2 ARC/GaAs solar cell interface

Furthermore, after the coating and substrate reach a prestress stage, as shown in figure 6, the principal stress begins to increase at the same arc length, rising from 0.08 MPa to 0.19 MPa. The 35years stress level is relatively almost to the initial stress observed in the first year. This compressive stress can create the large difference in Young's modulus between the coating and the solar cell which decreases the adhesive and strain energy store at the interface later resulted the imperfection and affecting the interface toughness. The toughness of the interface decreases from 0.25MPa to 0.01MPa after 35years under mechanical and thermal load. This indicate the presence of residual stress at the interface which leads to micro-cracks and delamination, leading to the excess stress extends to other components of the module. However, when stress reaches the solar cells, it used to damage the interconnections between the cells or even the solar cell.

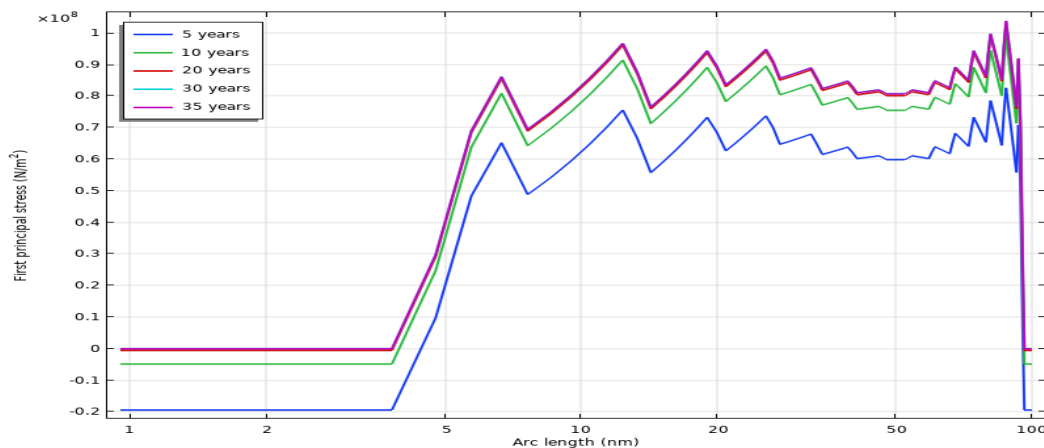


Figure 6: 35-years first principal stress distribution at interface of TiO_2 ARC/GaAs solar cell

Similarly, the deformation gradient at the interface during the first five years is minimal compared to the long-term deformation of 35years. As shown in figure 7, the deformation gradient grows from 100.23(%) to 100.90(%) uniformly at arc length of 8(nm) to 88(nm).

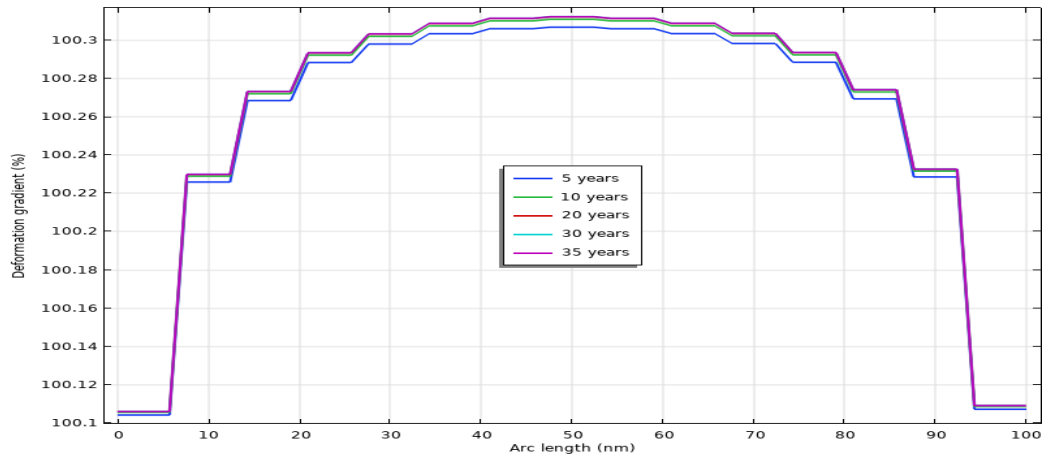


Figure 7: 35 years deformation gradient at interface of TiO_2 ARC/GaAs solar cell

The misalignment of Poisson ratio between the coating and solar cell materials increase the delamination risk where the magnitude of crack growth rate and propagation at both the surface and interface increases after 20 years. The centre (50nm) coating surface, interface and edges of the coating are the areas that experience the highest stress and most deformation as shown in figure 8a and 8b. This is because the module edge was set as a fixed constraint in order to account the module's frame structural effect, preventing full expansion and contraction, this results in the accumulation of stress and early deformation. Also, the mismatch in coefficient of thermal expansion between the two layers made the interface a stress spot. However, the reduction in thermal expansion experience by the coating lead the crack growth to propagate toward the stress spot as shown in Figure 8. Therefore, the higher the stress the higher the magnitude of crack propagation. The magnitude and direction of the arrows shown in Figure 8c indicate the points of crack growth direction and propagation.

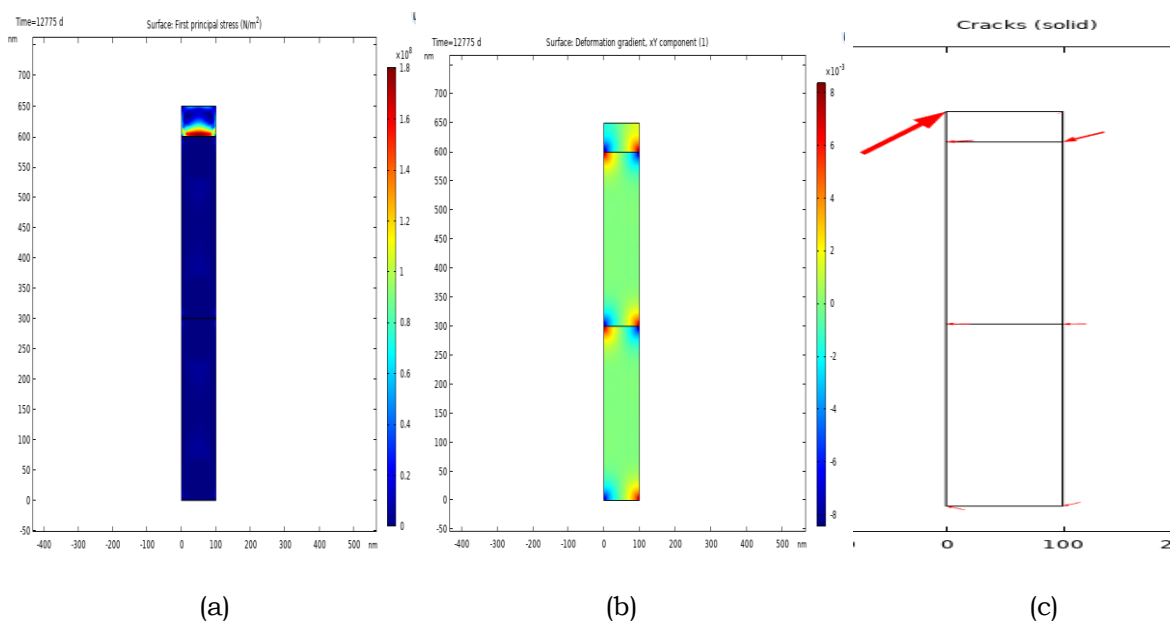


Figure 8: Two dimension of first principal stress, deformation and crack growth direction

CONCLUSION

We found that, under thermal and mechanical stress, the first principal stress at the coating surface and interface decreased over the first five years to 0.07MPa and 0.08MPa, respectively, before increasing to 0.145MPa and 0.19MPa after 35years. The deformation gradient during the first five years was negligible; however, significant deformation was observed at the coating surface (at arc length of 50nm), edge, and interface after 35years. By 35 years, the surface emissivity and interface toughness had decreased to 0.30 and 0.01MPa, respectively, indicating that the coating could no longer withstand additional stress. The crack growth direction magnitude reached 0.83%, with notable development at the coating edges and interface. These findings provide a valuable insight for analysing the long-term durability of PV modules exposed to outdoor environmental conditions. The results would also help solar module industries in design a durable module by selecting appropriate coating materials.

REFERENCES

- Arndt, R., & Robert Puto, I. (2010). *Basic Understanding of IEC Standard Testing for Photovoltaic Panels*.
- Eitner, U., Kajari-Schröder, S., Köntges, M., & Altenbach, H. (2011). Thermal stress and strain of solar cells in photovoltaic modules. *Advanced Structured Materials*, 15, 453–468. https://doi.org/10.1007/978-3-642-21855-2_29
- Gambogi, W., Kopchick, J., Felder, T., MacMaster, S., Bradley, A., Hamzavy, B., Yu, B.-L., Stika, K., Garreau-Iles, L., Fu Wang, C., Hu, H., Heta, Y., Trout, T.-J., DuPont de, E. I., & Co, M. (2015). *Multi-Stress Durability Testing to Better Predict Outdoor Performance of PV Modules*.
- Hasan, O., Arif, A. F. M., & Siddiqui, M. U. (2014). Finite element modeling, analysis, and life prediction of photovoltaic modules. *Journal of Solar Energy Engineering, Transactions of the ASME*, 136(2). <https://doi.org/10.1115/1.4026037>

- IEC. (2008). *INTERNATIONAL STANDARD NORME INTERNATIONALE Thin-film terrestrial photovoltaic (PV) modules-Design qualification and type approval Modules photovoltaïques (PV) en couches minces pour application terrestre-Qualification de la conception et homologation.*
- Jorgensen, G., Brunold, S., Köhl, M., Nostell, P., Roos, A., Oversloot, H., Jorgensen, G., Brunold, S., Köhl, M., Oversloot, H., & Roos, A. (1999). *Durability Testing of Antireflection Coatings for Solar Applications.* <http://www.doe.gov/bridgeonlineordering>:<http://www.ntis.gov/ordering.htm>
- Kempe, M. D., Hacke, P., Morse, J., Owen-Bellini, M., Holsapple, D., Lockman, T., Hoang, S., Okawa, D., Lance, T., & Ng, H. H. (2023). Highly Accelerated UV Stress Testing for Transparent Flexible Frontsheets. *IEEE Journal of Photovoltaics*, 13(3), 450–460. <https://doi.org/10.1109/JPHOTOV.2023.3249407>
- Leem, J. W., Su Yu, J., Jun, D. H., Heo, J., & Park, W. K. (2014). Efficiency improvement of III-V GaAs solar cells using biomimetic TiO₂ subwavelength structures with wide-angle and broadband antireflection properties. *Solar Energy Materials and Solar Cells*, 127, 43–49. <https://doi.org/10.1016/j.solmat.2014.03.041>
- Namvar, A., Dehghany, M., Sohrabpour, S., & Naghdabadi, R. (2016). Thermal residual stresses in silicon thin film solar cells under operational cyclic thermal loading: A finite element analysis. *Solar Energy*, 135, 366–373. <https://doi.org/10.1016/j.solener.2016.05.058>
- Noman, M., Tu, S., Ahmad, S., Zafar, F. U., Khan, H. A., Rehman, S. U., Waqas, M., Khan, A. D., & Rehman, O. ur. (2022). Assessing the reliability and degradation of 10–35 years field-aged PV modules. *PLoS ONE*, 17(1 January). <https://doi.org/10.1371/journal.pone.0261066>
- Owen-Bellini, M., Hacke, P., Miller, D. C., Kempe, M. D., Spataru, S., Tanahashi, T., Mitterhofer, S., Jankovec, M., & Topič, M. (2021a). Advancing reliability assessments of photovoltaic modules and materials using combined-accelerated stress testing. *Progress in Photovoltaics: Research and Applications*, 29(1), 64–82. <https://doi.org/10.1002/pip.3342>
- Owen-Bellini, M., Hacke, P., Miller, D. C., Kempe, M. D., Spataru, S., Tanahashi, T., Mitterhofer, S., Jankovec, M., & Topič, M. (2021b). Advancing reliability assessments of photovoltaic modules and materials using combined-accelerated stress testing. *Progress in Photovoltaics: Research and Applications*, 29(1), 64–82. <https://doi.org/10.1002/pip.3342>
- Raquel, J., & Ângelo, M. (2016). *Development and Characterization of Titania-based Photocatalysts and their Incorporation in Paint Coatings.*
- Rezaei, B., & Mosaddeghi, H. (2006). *Applications of Titanium Dioxide Nanocoating.*
- Wohlgemuth, J. H., & Kempe, M. D. (2013). *Equating Damp Heat Testing with Field Failures of PV Modules.*
- Zäll, E., Karlsson, S., Järn, M., Segervald, J., Lundberg, P., & Wågberg, T. (2023). Durability of antireflective SiO₂ coatings with closed pore structure. *Solar Energy Materials and Solar Cells*, 261. <https://doi.org/10.1016/j.solmat.2023.112521>
- Zeng, Y., Song, N., Lim, S., Keevers, M., Wu, Y., Yang, Z., Pillai, S., Jiang, J. Y., & Green, M. (2023). Comparative durability study of commercial inner-pore antireflection coatings and alternative dense coatings. *Solar Energy Materials and Solar Cells*, 251. <https://doi.org/10.1016/j.solmat.2022.112122>